CellPress

Cell Host & Microbe
Article

PLEKHM1 Regulates *Salmonella*-Containing Vacuole Biogenesis and Infection

David G. McEwan,[1] Benjamin Richter,[1] Beatrice Claudi,[2] Christoph Wigge,[3] Philipp Wild,[1] Hesso Farhan,[2,4] Kieran McGourty,[5] Fraser P. Coxon,[6] Mirita Franz-Wachtel,[7] Bram Perdu,[8] Masato Akutsu,[2] Anja Habermann,[3] Anja Kirchof,[1] Miep H. Helfrich,[6] Paul R. Odgren,[9] Wim Van Hul,[8] Achilleas S. Frangakis,[2] Krishnaraj Rajalingam,[10] Boris Macek,[7] David W. Holden,[5] Dirk Bumann,[2,*] and Ivan Dikic[1,3,11,*]

[1]Institute of Biochemistry II, Goethe University School of Medicine, Theodor-Stern-Kai 7, D-60590 Frankfurt (Main), Germany
[2]Infection Biology, Biozentrum, University Basel, Klingelbergstr. 50/70, CH-4056 Basel, Switzerland
[3]Buchmann Institute for Molecular Life Sciences, Max-von-Laue-Str. 15, Goethe University 60438 Frankfurt am Main, Germany
[4]Biotechnology Institute Thurga, Department of Biology, University of Konstanz, 78457 Konstanz, Germany
[5]Centre for Molecular Microbiology and Infection, Imperial College London, Armstrong Road, London SW7 2AZ, UK
[6]Musculoskeletal Research Programme, Division of Applied Medicine, Institute of Medical Sciences, University of Aberdeen, Foresterhill, Aberdeen AB25 2ZD, UK
[7]Proteome Center Tübingen, Interfaculty Institute for Cell Biology, University of Tübingen, Auf der Morgenstelle 15, 72076 Tübingen, Germany
[8]Department of Medical Genetics, University of Antwerp, Prins Boudewijnlaan 43B, 2650 Edegem, Belgium
[9]Deptartment of Cell Biology, S7-242, University of Massachusetts Medical School, North Worcester, MA 01655, USA
[10]Molecular Signaling Unit, FZI, Institute for immunology, University Medical Center of the Johannes Gutenberg-University Mainz, Langenbeckstraße 1, Mainz 55131, Germany
[11]University of Split, School of Medicine, Department of Immunology and Medical Genetics, Soltanska 2, 21 000 Split, Croatia
*Correspondence: dirk.bumann@unibas.ch (D.B.), Ivan.Dikic@biochem2.de (I.D.)
http://dx.doi.org/10.1016/j.chom.2014.11.011

SUMMARY

The host endolysosomal compartment is often manipulated by intracellular bacterial pathogens. *Salmonella* (*Salmonella enterica serovar* Typhimurium) secrete numerous effector proteins, including SifA, through a specialized type III secretion system to hijack the host endosomal system and generate the *Salmonella*-containing vacuole (SCV). To form this replicative niche, *Salmonella* targets the Rab7 GTPase to recruit host membranes through largely unknown mechanisms. We show that Pleckstrin homology domain-containing protein family member 1 (PLEKHM1), a lysosomal adaptor, is targeted by *Salmonella* through direct interaction with SifA. By binding the PLEKHM1 PH2 domain, *Salmonella* utilize a complex containing PLEKHM1, Rab7, and the HOPS tethering complex to mobilize phagolysosomal membranes to the SCV. Depletion of PLEKHM1 causes a profound defect in SCV morphology with multiple bacteria accumulating in enlarged structures and significantly dampens *Salmonella* proliferation in multiple cell types and mice. Thus, PLEKHM1 provides a critical interface between pathogenic infection and the host endolysosomal system.

INTRODUCTION

Salmonella enterica (henceforth *Salmonella*) is a facultative intracellular pathogen that causes acute gastroenteritis or life-threatening systemic infections (enteric fever) in humans. After host cell invasion, it resides within membrane-bound *Salmonella*-containing vacuoles (SCVs) and injects virulence factors into the cell cytosol to regulate host proteins, including the small GTPase Rab7 and the lysosomal protein marker LAMP1 (Gorvel and Meresse, 2001; Méresse et al., 1999; Patel and Galán, 2005; Ramsden et al., 2007). As part of the endolysosomal membrane network, Rab7 activation is achieved by HOPS complex and other guanine-nucleotide exchange factors such as Mon/Ccz1 (Nordmann et al., 2010; Peralta et al., 2010). *Salmonella* proliferates within this newly established intracellular niche protected from the immune competent cytosol of the host cell. By contrast, upon SCV membrane rupture, *Salmonella* can be marked with ubiquitin or diacylglycerol resulting in the autophagic elimination of cytosol-exposed bacteria (Birmingham et al., 2006; Gomes and Dikic, 2014; Shahnazari et al., 2010). Central to the survival of the bacteria inside the host is the maintenance of the integrity of the SCV and formation of *Salmonella*-induced filaments (Sifs), which require a continuous supply of membranes. The Rab family of small guanine nucleotide-binding proteins are crucial regulators of membrane trafficking within the cell, and Rab effector proteins including kinases, tethering factors, and motor proteins play important roles in the pathogenesis of microbial infections (Stenmark, 2009). For instance, Gram-negative bacteria such as *Salmonella* hijack Rab7 function to modify SCV maturation (Méresse et al., 1999) and to facilitate dynein-mediated centripetal displacement of *Salmonella* toward the microtubule organizing center (MTOC) (Guignot et al., 2004; Harrison et al., 2004). Rab7 is targeted by multiple intracellular pathogens, including *Coxiella burnetti* (Berón et al., 2002) and *Helicobacter pylori* (Papini et al., 1994), but is actively blocked by *Mycobacterium tuberculosis*, which remain in an early endosomal compartment positive for Rab5 (Via et al., 1997). Thus, a diverse array of strategies aid pathogen manipulation of the

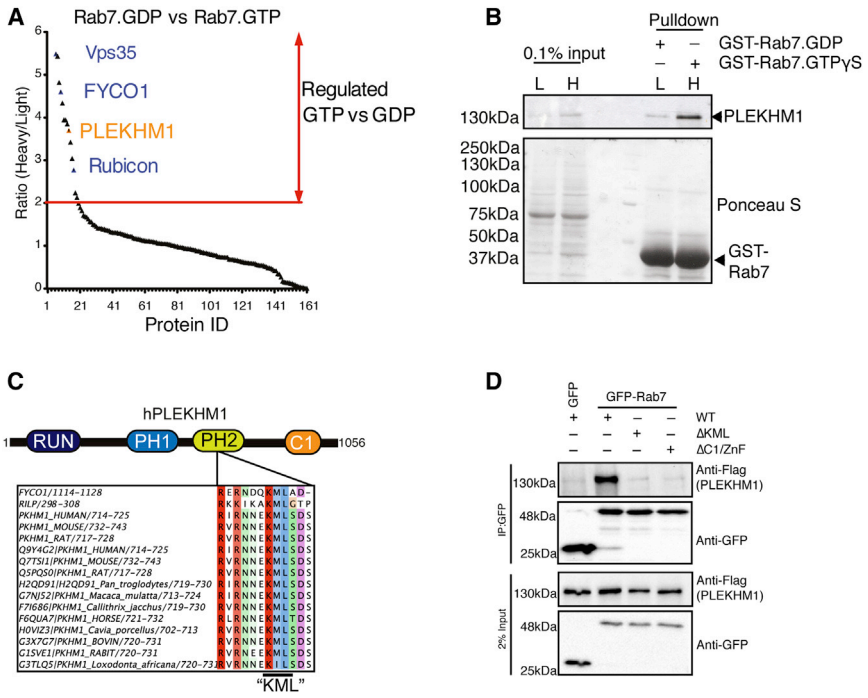

Figure 1. PLEKHM1-PH2 Domain Regulates PLEKHM1-Rab7 Interaction

(A) GST-Rab7-precipitated interaction partners ranked with a descending order of normalized H/L ratio. H/L ratio > 2 was regarded as regulated GTP versus GDP (red line). Rab7 interaction partners are highlighted (blue = known; orange = PLEKHM1).

(B) Samples from the pulldowns carried out in (A) were tested for the presence of endogenous PLEKHM1 using an antibody raised against aa 626–642 of human PLEKHM1 protein.

(C) Sequence alignment of hRILP (aa 294–308), hFYCO1 (aa 1,114–1,128), and PLEKHM1 PH2 from multiple species. The conserved KML (aa 720–722 PLEKHM1) motif is highlighted.

(D) Coimmunoprecipitation of either GFP alone or GFP-Rab7 WT with PLEKHM1-WT-FLAG or mutants. All blots and images are representative of at least n = 3 experiments. See also Figure S1 and S2 and Tables S1 and S2.

host endolysosomal system to create a suitable intracellular niche for replication and survival.

Salmonella effector proteins, such as *Salmonella*-induced filament protein A (SifA), are translocated into the host endomembrane system and cytosol mediating membrane recruitment to the growing SCV (Beuzón et al., 2000; Stein et al., 1996). One SifA effector, SifA and kinesin-interacting protein (SKIP), interacts directly with SifA and Rab9 (but not Rab7) via its pleckstrin homology (PH) domain, is required for kinesin recruitment and *Salmonella* pathogenesis, and SifA through SKIP depletes host cells of lysosomal degradative enzymes by inhibiting Rab9-dependent retrograde trafficking of mannose-6-phosphate receptors (Boucrot et al., 2005; Diacovich et al., 2009; Dumont et al., 2010; Jackson et al., 2008; McGourty et al., 2012; Ohlson et al., 2008). SifA has been suggested to recruit Rab7 via uncoupling Rab7 from Rab7-interacting lysosomal protein (RILP); however, no direct interaction between SifA and Rab7 has been shown (Harrison et al., 2004; Jackson et al., 2008), indicating that another factor may be involved in linking SifA with Rab7 function.

We therefore set out to identify interactions between SifA and host proteins for the recruitment of Rab7. In a stable isotope labeling of amino acids (aa) in cell culture (SILAC)-based mass spectrometry (MS) analyses, we found PH and RUN-domain containing protein 1 (PLEKHM1) as a specific interactor of active Rab7 GTPase as well as HOPS complex (McEwan et al., 2015). We show that PLEKHM1 is a direct target of *Salmonella*, interacting with SifA through the second PH domain (PH2). The SifA-PLEKHM1 interaction is required by the pathogen to recruit endolysosomal membrane pools that are essential for the growth of the SCV and proliferation in primary cells and tissues from infected mice. Furthermore, reconstitution with wild-type (WT) PLEKHM1 rescued SCV morphology, while SifA interaction mutants displayed abnormal "bag-like" SCVs similar to those observed after PLEKHM1 HOPS or Rab7 depletion. These findings indicate that PLEKHM1 regulates SifA-dependent *Salmonella* vacuole dynamics in concert with the HOPS complex and Rab7.

RESULTS

PLEKHM1 Is an Adaptor for Rab7

To screen Rab7 interaction partners in a dynamic and comparative way, we performed a SILAC-based MS analysis. Purified GST-tagged Rab7, preloaded with either GDP (inactive) or GTPγS (active), was incubated with (Arg0 and Lys0) LIGHT- or (Arg10 and Lys8) HEAVY-labeled HeLa cell lysates, respectively (Figure S1A available online). Subsequent MS analysis revealed a total of 203 interacting proteins (161 quantified), with 17 displaying heavy/light (H/L) ratios ≥2 (Figure 1A, red line; Rab7.GTP enriched). We found PLEKHM1 as a preferential interacting partner of GTPγS-loaded Rab7 (Figurse 1A, S1B, and S1C; Table S1; H/L ratio 3.7), along with other known Rab7-interacting proteins (Figure 1A; Blue), including FYCO1 (Pankiv et al., 2010), Vps35 (Seaman et al., 2009), and Rubicon (Sun et al., 2010; Tabata et al., 2010) (Figure 1A). Using an antibody raised against human PLEKHM1, we confirmed that endogenous PLEKHM1 is enriched specifically in the Rab7.GTPγS fraction (Figure 1B). We found that PLEKHM1 specifically interacted with Rab7 but not Rab9 or other late endocytic or recycling Rabs (Figure S2A).

In mapping the interaction between PLEKHM1 and Rab7, only regions of PLEKHM1 that contained both the PH2 domain and C1/ZnF were able to coprecipitate and colocalize with Rab7, while neither domain in isolation was able to do so (Figures S2B and S2C). Sequence analysis of the PH2 domain revealed a highly conserved Lys-Met-Leu (KML) motif (Figure 1C; Table S2) that was essential for the interaction and colocalization with Rab7 (Figures 1D and S2D). Moreover, using GST-RILP to

precipitate the active (GTP-bound) fraction of Rab7 (Figure S2E) (Sun et al., 2009), we observed stabilization of endogenous Rab7.GTP only in PLEKHM1-WT but not in Rab7-interaction (-ΔKML or -ΔC1/ZnF) mutant cells (Figure S2F). In agreement, depletion of PLEKHM1 led to a reduction of Rab7.GTP levels by approximately 60% (Figures S2G and S2H). This indicated that Rab7 interaction with PLEKHM1 is essential for preserving active pools of Rab7 in cells.

PLEKHM1 Localization at the Lysosome Is Dependent on Both Rab7 and HOPS

To gain a better understanding of PLEKHM1 function, we performed MS analysis of PLEKHM1 interaction partners and identified multiple components of the homotypic fusion and vacuole protein sorting (HOPS) complex (McEwan et al., 2015). These interactions indicated that PLEKHM1 acts as a specific adaptor molecule for Rab7-HOPS complex and that PLEKHM1 might be mutually regulated in such a trimeric complex. We therefore wanted to address how PLEKHM1 positioning at the lysosome may be affected in the absence of HOPS and Rab7.

Stable overexpression of PLEKHM1-GFP in U20S cells induced the formation of enlarged, clustered vesicles that were positive for both Rab7 and LAMP2 ($Rab7^{+}$/$LAMP2^{+}$) and formed two distinct subpopulations: a tightly associated cluster of vesicles at the perinuclear region (Figure 2Ai) and individual or pairs of vesicles localized toward the cell periphery (Figure 2Aii). These vesicles may represent subpopulations of lysosomes at different states of activation, as lysosomes traffic toward the cell periphery under nutrient-rich conditions and toward the perinuclear regions during starvation (Korolchuk et al., 2011). Next, to confirm these were lysosomes, we performed a pulse chase experiment using fluorescently labeled dextran. Cells were incubated with Alexa 647-labeled dextran and allowed it to traffic to the lysosomes (>3 hr). Next, we pulsed for 15 min with Alexa 555 dextran; washed and replaced the growth media; and allowed the experiment to proceed for 0, 30, 60, and 180 min prior to fixation of cells (Figure S3A). We observed a time-dependent increase in Alexa555 dextran staining of PLEKHM1 vesicles, particularly at the later time points (180 min) indicating trafficking to the lysosome, whereas the dextran647 colocalization did not vary greatly over time, indicating its presence in the lysosome (Figures S3B–S3D). Thus, we propose that PLEKHM1 resides mainly on the lysosomes with LAMP2 and Rab7.

Next, transient siRNA-mediated depletion of Rab7 (Figure 2B; siRab7) caused a profound dispersal of the PLEKHM1-positive vesicles and significantly ablated the colocalization with LAMP2 (Figures 2B and 2E) with only a few small PLEKHM1/LAMP2 puncta evident (Figure 2B, ROI enhancement, arrow heads). Loss of hVps41, a component of HOPS complex, fragmented PLEKHM1 vesicles into smaller punctate structures and also affected PLEKHM1 colocalization with both Rab7 and LAMP2, but not as severely as Rab7 depletion (Figures 2C and 2E). Silencing of exogenous and endogenous PLEKHM1 caused a dispersal of both Rab7 and LAMP2 signals, with the latter forming smaller vesicles (Figure 2D; Table S3), indicating that the enlarged lysosomes observed were induced by PLEKHM1 overexpression. Furthermore, depletion of Rab7 (Figure 2F) or mutation of the Rab7 interaction surfaces (Figure S3E) diminished PLEKHM1 coprecipitation with hVps41, indicating a dependency on Rab7 for hVps41 interaction. Taken together, these data suggest that PLEKHM1 primarily interacts with Rab7 and depletion of either Rab7 or HOPS complex disturbs PLEKHM1 localization at the lysosome.

Salmonella Intracellular Proliferation Requires PLEKHM1

Salmonella vacuole biogenesis is dependent upon the endocytic-like maturation of a spacious vacuole to one localized at the MTOC, which retains LAMP1/LAMP2 and CD63 proteins and extrudes large filamentous extensions, or Sifs (Figure S4A) (Dumont et al., 2010; Guignot et al., 2004; McGourty et al., 2012; Méresse et al., 1999; Steele-Mortimer et al., 1999). Ruptured SCVs allow *Salmonella* to hyperproliferate in the host cytosol (Figure S4A). Thus, we tested the effect of PLEKHM1 depletion on *Salmonella* proliferation using colony-forming units (cfu) as a measurement of intracellular proliferation. *Salmonella* infection of shCntrl HeLa cells resulted in continuous intracellular growth, with approximately 15-fold increase at 24 hr postinfection (p.i.) (Figure S4B); however, shRNA depletion of PLEKHM1 resulted in a statistically significant 2- to 2.5-fold diminished *Salmonella* growth (Figures 3A and S4B) that mirrored by Rab7 depletion (Figure 3B; siRab7#2 and siRab7#3). Consistently, we observed similar levels of decreased *Salmonella* proliferation in primary *Plekhm1*$^{-/-}$ mouse embryonic fibroblasts (MEFs) (Figure 3C) and *Plekhm1*$^{-/-}$ primary macrophages derived from the peritoneal cavity (Figure 3D) compared to *Plekhm1*$^{+/+}$ cells, respectively. We then tested whether genetic loss of *Plekhm1* in mice affected in vivo proliferation. Next, age-matched *Plekhm1*$^{+/+}$ and *Plekhm1*$^{-/-}$ mice were infected with WT Salmonella (SL1344) by intravenous injection, and the livers and spleens were harvested 5 days p.i., and cfu counts were analyzed. Intravenous infection of *Plekhm1*$^{-/-}$ mice resulted in a moderate, but statistically significant, decrease in *Salmonella* proliferation in both the spleen and liver of infected animals, compared to congenic C57BL/6 mice (Figures 3E and 3F). Overall, these results confirmed that PLEKHM1 is a regulator of *Salmonella* proliferation in multiple cell types and is required for efficient infection of mice.

PLEKHM1 and SifA Form a Functional Complex in Infected Cells

Next, we sought to understand how PLEKHM1 influences *Salmonella* proliferation in cells. Overexpression of PLEKHM1 revealed that PLEKHM1 localizes with LAMP1 to distinct regions of the SCV during infection (Figure 4A, arrow heads). SifA is an essential, SCV localized, bacterial effector protein for *Salmonella* virulence, Sif formation, and SCV integrity (Jackson et al., 2008; Ohlson et al., 2008) and is essential for systemic infection (Beuzón et al., 2000; Stein et al., 1996). PLEKHM1 shares a similar domain structure to SKIP, which was previously shown to localize and interact with SifA (Diacovich et al., 2009). Surprisingly, we found that PLEKHM1, similar to SKIP, could colocalize with 2xHA-epitope-tagged SifA (S12023-2HA-SifA) at the SCV (Figure 4B; ROI, arrow heads) and with SifA that was not associated with the SCV but present on vesicles (Figure 4B, open arrows). We could coprecipitate PLEKHM1 and endogenous Rab7 with 2xHA-SifA from an infected PLEKHM1-inducible cell line at 16 hr p.i. (Figure 4C) but not from noninfected cells.

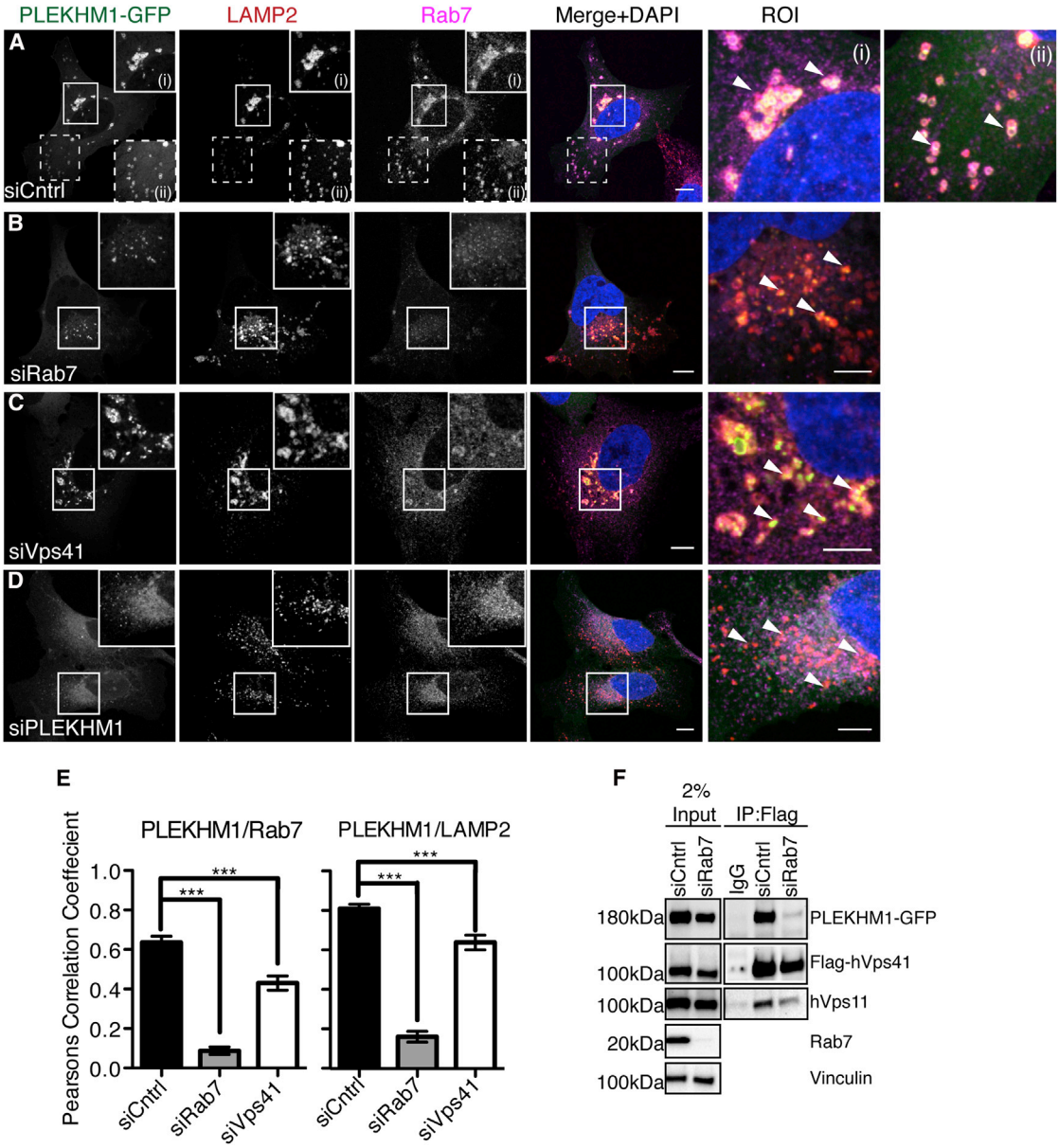

Figure 2. PLEKHM1, Rab7 and Vps41 Coordinate Lysosome Tethering

(A–D) (A) U2OS PLEKHM1-WT-GFP (green) cells were treated with either nontargeting controls siRNA (siCntrl) or siRNA against Rab7 (siRab7; [B]), hVps41 (siVps41; [C]), or PLEKHM1 (siPLEKHM1, [D]). Endogenous LAMP2 (red) Rab7 (magenta) and DAPI (nucleus, blue) were stained. Boxed regions are shown as enhanced region of interest (ROI). Scale bar 10 μm

(E) Pearson's correlation coefficient analysis of PLEKHM1/Rab7 and PLEKHM1/LAMP2 of (A)–(C). Mean ± SEM of n = 150 cells per condition. ***p < 0.0003.

(F) Immunoprecipitation of hVps41 and PLEKHM1 from HEK293T cells transfected with siCntrl or siRab7 and PLEKHM1-WT-GFP plus Flag-hVps41. Antibodies to GFP (PLEKHM1), Flag (hVps41), Rab7, and Vinculin were used. See also Figure S3 and Table S3.

Therefore, we hypothesized that PLEKHM1, SifA, and Rab7 formed a trimeric complex in cells. Concordantly, SifA only co-precipitated with Rab7 in the presence of PLEKHM1-WT and not with any mutant of PLEKHM1 that fails to interact with Rab7 (ΔPH2, ΔKML, or ΔC1/ZnF; Figure 4D). Thus, PLEKHM1 and SKIP (PLEKHM2) may represent a class of related proteins being used by *Salmonella*, through SifA, to manipulate the endo-lysosomal system.

PLEKHM1 Interacts Directly with SifA

Next, we were interested to test whether PLEKHM1 interacted with SifA. PLEKHM1 readily coprecipitated with SifA but not the related protein SifB (Figure 5A). Indeed, full-length maltose-binding protein (MBP)-tagged PLEKHM1 purified from *E.coli* lysates interacted directly with GST-tagged SifA and GST-GABARAP (McEwan et al., 2015) but not GST alone or GST-SifB (Figure 5B). Thus, PLEKHM1 interacts directly

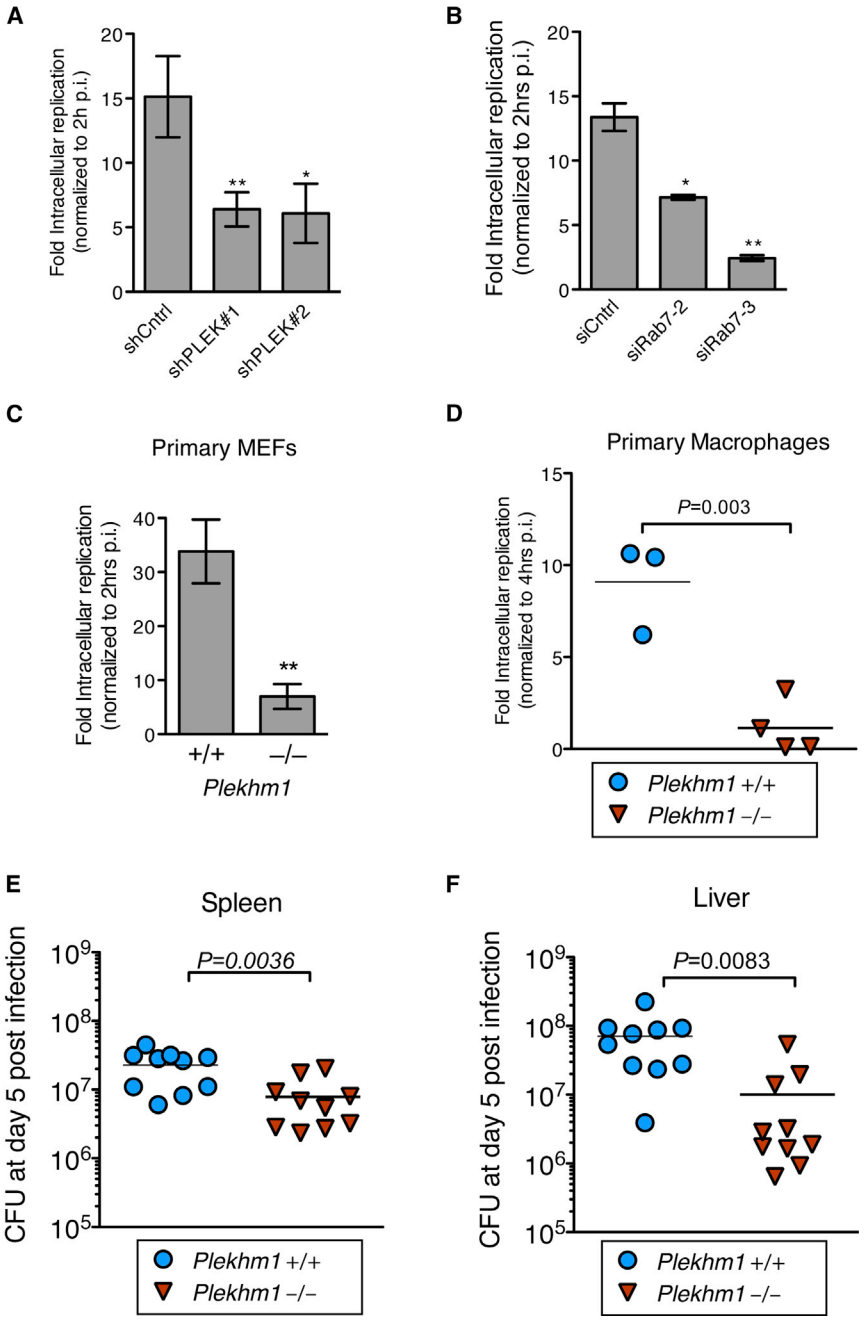

Figure 3. Loss of PLEKHM1 Inhibits *Salmonella* Proliferation

(A) shCntrl and shPLEKHM1 (shPLEK#1 and shPLEK#2) HeLa cell lines were infected with WT *Salmonella* (SL1344), lysed at 2 and 24 hr p.i., and bacterial colonies were counted on selective agar plates. Cfu counts normalized to 2 hr p.i. Mean of n = 3 independent experiments ± SD. **p = 0.0037; *p = 0.0158 compared to shCntrl. Unpaired t test.

(B) SL1344 *Salmonella* proliferation in HeLa cells at 24 hr p.i. and 72 hr after Rab7 depletion using two different siRNAs. Cfu shown as fold change compared to 2 hr p.i. Error bars represent mean ± SD of n = 3 independent experiments. **p < 0.005; *p < 0.02. Unpaired t test.

(C) Cfu counts (fold 2 hr p.i.) of Plekhm1 WT (*Plekhm1*$^{+/+}$) and Plekhm1 knockout (*Plekhm1*$^{-/-}$) primary MEFs. Error bars represent mean ± SD of n = 3 independent experiments. **p = 0.0028; unpaired t test

(D) Macrophages derived from the peritoneal cavity (PDM) of *Plekhm1*$^{+/+}$ (blue circle) and *Plekhm1*$^{-/-}$ mice (red triangle) infected with *Salmonella* (SL1344) grown overnight to saturation and cfu measured at 24 hr p.i. Results expressed as fold change from 4 hr p.i. Single shapes represent macrophages from individual mice. **p = 0.003 unpaired t test.

(E and F) (E) *Plekhm1*$^{+/+}$ C57BL/6 (blue circle) or congenic *Plekhm1*$^{-/-}$ (red inverted triangle) littermate mice were intravenously infected with approximately 1,300 cfu WT *Salmonella* SL1344 and sacrificed at day 5 p.i. Ten animals were used per condition. Spleens (E) and livers (F) were isolated and the cfu measured. Statistical analysis with unpaired t test where p < 0.05 was deemed significant. p = 0.0036 (E); **p = 0.0083 (F). See also Figure S4.

with SifA. Indeed, the PLEKHM1-SifA interaction was dependent upon the second PH domain of PLEKHM1 (PH2; Figure 5C), and the N-terminal domain of SifA (aa 1–140; Figure S5A). In addition, interaction with the N-terminal domain of SifA could be out-competed to a certain degree with increasing concentrations of SKIP, indicating that PLEKHM1 and SKIP interact with SifA through a similar surface (Figure S5B). Coexpression of both SKIP and PLEKHM1 in the absence of SifA showed little overlapping colocalization (Figure S5C), suggesting that they operate in functionally distinct compartments. Site-directed mutagenesis of the PH2 domain identified three residues, E729, T730, and R769, that when mutated to alanine disrupted PLEKHM1 interaction with SifA (Figures 5D and S5D). Importantly, neither E729A nor R769A mutations affected PLEKHM1-Rab7 interaction or colocalization (Figures S6A–S6C), despite their proximity to the KML motif. Thus, the SifA (E729 and R769) and Rab7 ("KML" motif, aa 720–722) interaction regions of PLEKHM1-PH2 domain represent mutually exclusive surfaces that may facilitate simultaneous binding of both Rab7 and SifA. Therefore, we generated a molecular model of the complex containing PLEKHM1-PH2 domain and both SifA and Rab7. To generate our model, we used the SKIP-PH-SifA structure (PDB: 3CXB), the Sec3-PH domain (PDB:3A58) complexed with Rho GTPase, and phosphatidylinositol via two distinct surfaces, Rab7 alone (PDB: 1T91) and Rab7:RILP (PDB: 1YHN), which was superimposed on the Rho GTPase structure. Using the information at hand, we hypothesized that the PLEKHM1-PH2 (magenta/blue; center) can interact simultaneously with both SifA (right) and Rab7 (left). K720 of the PH2 domain is orientated toward the corresponding RILP K304 binding site

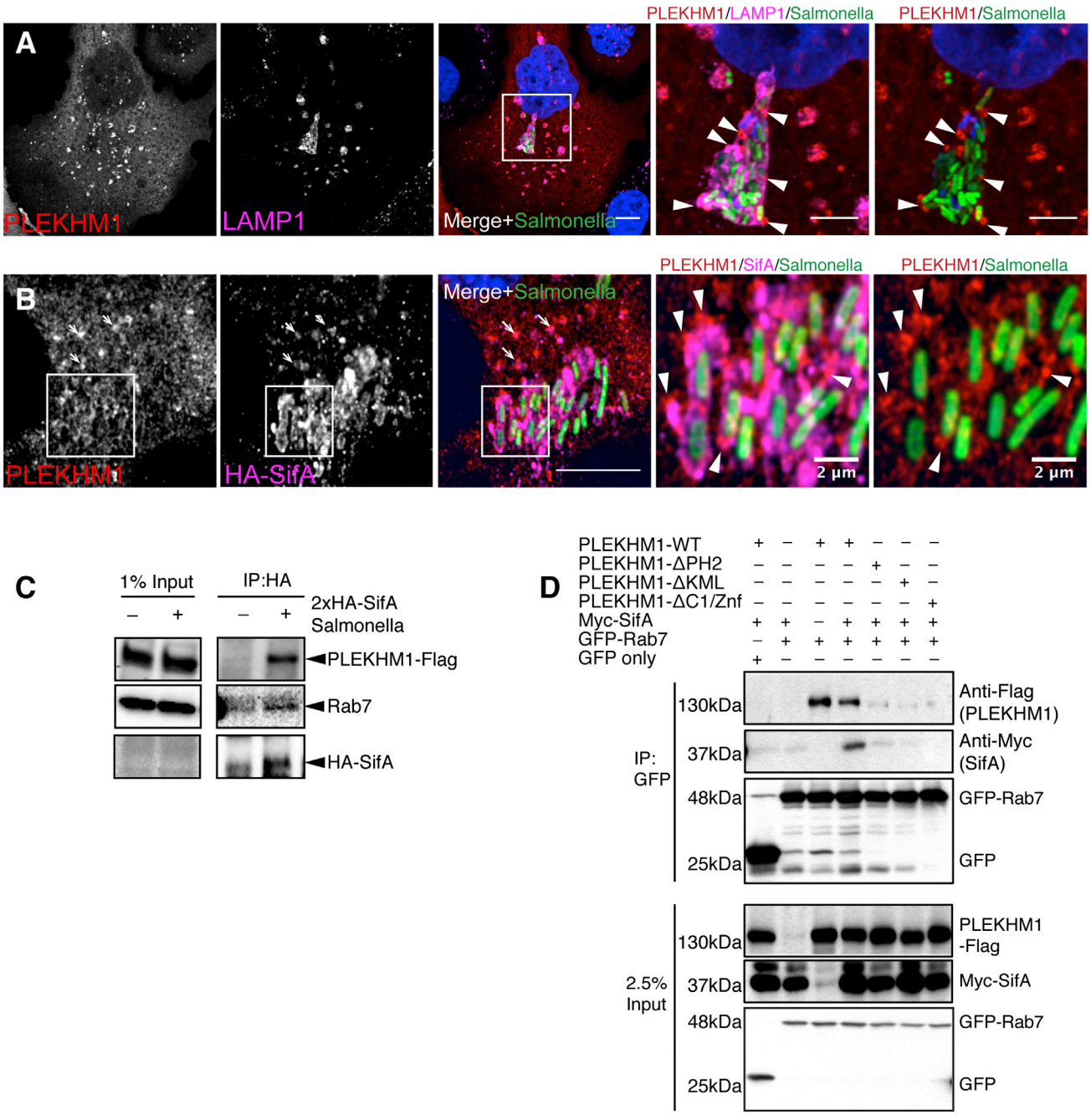

Figure 4. PLEKHM1 Localizes with SifA in Proximity to the SCV

(A) PLEKHM1 shRNA-depleted cells were transiently transfected with shRNA-resistant PLEKHM1-WT-2xFlag, infected with GFP-expressing WT *Salmonella* (SL1344), fixed at 20 hr p.i., and stained with Anti-PLEKHM1 (PLEKHM1;Red) and anti-LAMP1 (magenta). DAPI (blue) and GFP-Salmonella (green) is shown in the merged image. Boxed regions are enhanced in the panels labeled ROI. Arrows indicate structures of interest. Scale bars 10 μm (large cells) and 2 μm (ROI).

(B) *Salmonella* expressing 2xHA-tagged SifA (pACYC-sifa-2HA)-infected Myc- PLEKHM1 HeLa cells at 14 hr p.i. stained for the presence of Myc-PLEKHM1 (red) and HA(SifA; magenta). Enhancements of boxed regions shown for clarity. Arrows indicate structures of interest. Scale bars 10 μm.

(C) Immunoprecipitation of 2xHA-SifA from noninfected or *Salmonella*-infected PLEKHM1-2xFlag HeLa Flp-In T-REx 14h p.i. Anti-Flag (PLEKHM1), anti-Rab7, and anti-HA was probed. HA-SifA was only detected in the precipitated fraction due to low levels of expression.

(D) Immunoprecipitation of GFP-Rab7-WT with Myc-SifA in the presence or absence of PLEKHM1-WT-Flag or PLEKHM1 Rab7 interaction mutants (PLEKHM1-ΔKML, -ΔPH2 or -ΔC1/ZnF). Samples were probed for the presence of PLEKHM1 (Flag), Myc (SifA), and GFP (Rab7).

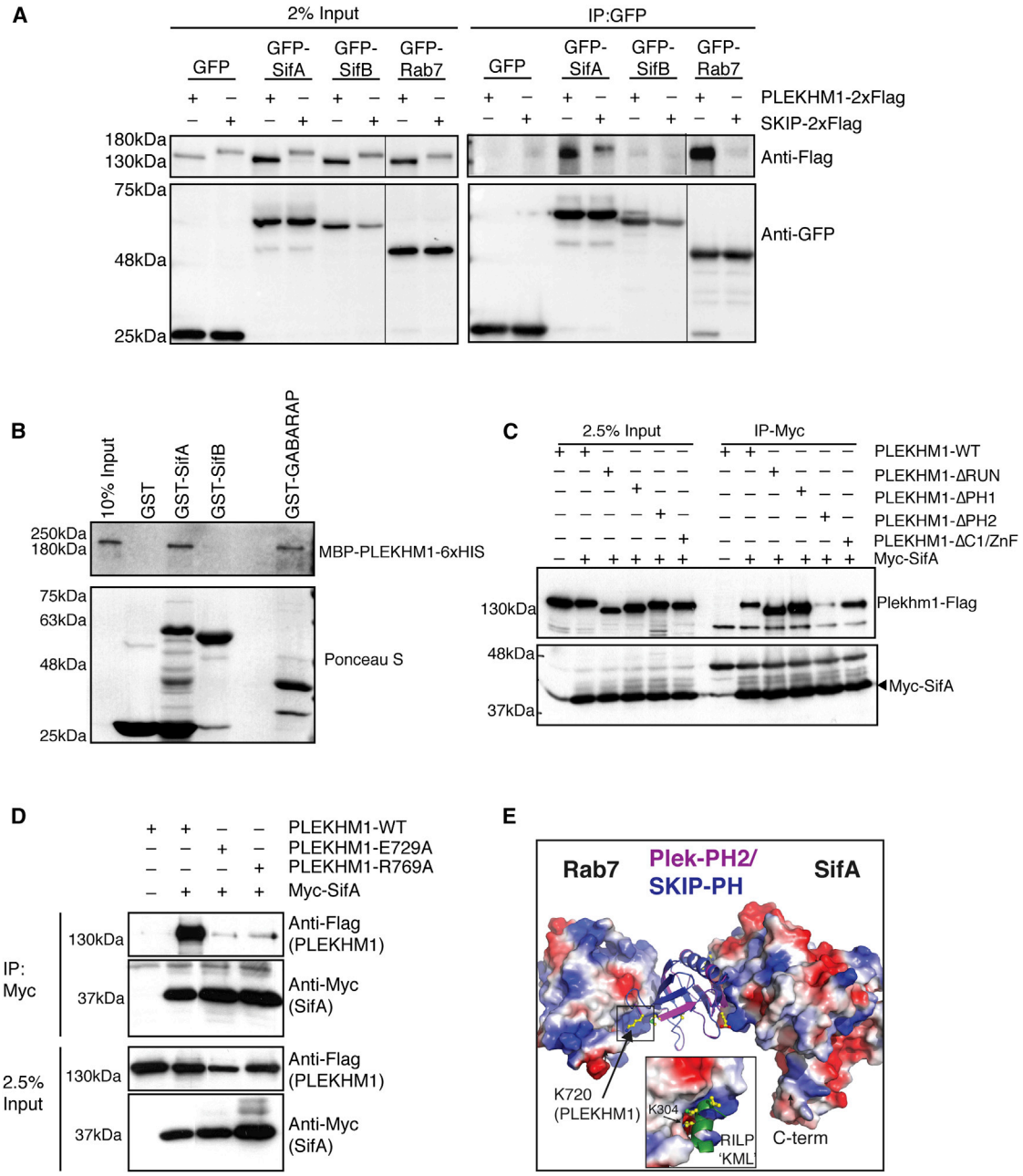

Figure 5. PLEKHM1 Interacts with SifA through Its PH2 Domain

(A) Coimmunoprecipitation of either Plekhm1-2xFlag or SKIP-2xFlag cotransfected GFP alone, GFP-SifA, GFP-SifB, or GFP-Rab7 from uninfected HEK293T cells. GFP was precipitated using anti-GFP trap beads.

(B) GST pull-down of recombinant MBP-tagged PLEKHM1-6xHIS with GST alone, GST-SifA, GST-SifB, and GST-GABARAP.

(C) Coimmunoprecipitation Myc-SifA with PLEKHM1 domain deletion mutants.

(D) Immunoprecipitation of Myc-tagged SifA (WT) from noninfected HEK293T cells with PLEKHM1-WT-Flag, PLEKHM1-E729A-, or PLEKHM1-R769A-Flag.

(E) PLEKHM1-PH2 was modeled on the SKIP-PH (PDB: 3CXB), and the Sec3-PH domain (PDB:3A58) interaction with the GTPase Rho and phosphatidylinositol via two distinct surfaces. Rab7 alone (PDB: 1T91) and Rab7:RILP (PDB: 1YHN) interaction was overlaid on the Rho GTPase structure. PLEKHM1-PH2 (magenta/blue; center) can potentially interact with both SifA (right) and Rab7 (left). K720 is orientated toward the corresponding RILP K304 binding site on Rab7 (boxed region; inset), and the C-terminal tails of Rab7 and SifA are orientated in the same direction for insertion into the same membrane. See also Figures S5 and S6.

on Rab7 (boxed region; inset), and the E729 and R769 of PLEKHM1 show corresponding interactions with the SifA-SKIP interaction surface (Figure 5E). Thus, we propose that PLEKHM1-PH2 domain can directly interact with both Rab7 and SifA to facilitate recruitment to SCVs and/or Sifs.

PLEKHM1 Regulates Membrane Biogenesis of the *Salmonella*-Containing Vacuole

Based on the above results, we hypothesized that PLEKHM1 may act as an adaptor platform for the regulation of SCV membrane dynamics.

HeLa shCntrl and shPLEKHM1 cells were infected with GFP-expressing *Salmonella* (SL1344-GFP), fixed at 20 hr p.i., and labeled for the SCV marker protein LAMP1. Control cells displayed large *Salmonella* microcolonies with 75.5% ± 2.0% of *Salmonella* residing within individual LAMP1 vacuoles with extended Sifs (Figures 6A and 6C). In contrast, more than 70% of GFP-*Salmonella*-infected, PLEKHM1-depleted cells displayed multiple *Salmonella* ($\geq$4) within a single enlarged vacuole characterized by a ring of LAMP1 (Figure 6B) and significantly fewer Sifs compared to control cells (Figure 6C). Indeed, no individual LAMP1-positive vacuoles were discernable by optical z stack analysis (Movie S1) or by electron micrograph (EM) images of infected shPLEKHM1 cells (Figure 6Dii, boxed area and arrows), compared to the tightly associated individual vacuoles in shCntrl cells (Figure 6Di, boxed area and arrows). Quantification of random EM sections showed approximately 63% ± 3.8% of shPLEKHM1-infected cells had >4 *Salmonella* per vacuole, compared to 34% ± 6.9% in shCntrl cells (Figure 6E). Live imaging of GFP-Salmonella-infected mCherry-LAMP1 expressing shCntrl, shPLEKHM1, or siRab7 HeLa cells revealed that the "bags" were generally static and showed very little movement, and no Sifs could be seen emanating from the *Salmonella* microcolony (Figures S7B and S7C; Movies S3 and S4), in stark contrast to the extensive and highly dynamic Sif networks present in the shCntrl HeLa (Figure S7A; Movie S2).

The regulation of PLEKHM1 localization and function is tightly linked to that of Rab7 and HOPS complex, as already indicated above. In accordance, depletion of Rab7 (Figure 6G), hVps41 (Figure 6H), hVps39 (Figure 6I), or hVps11 (Figure 6J) all resulted in a similar phenotype of altered SCV morphology (i.e., a bag of multiple *Salmonella* contained within a ring of LAMP1). These findings indicate that PLEKHM1 regulates *Salmonella* vacuole dynamics in concert with the HOPS complex and Rab7, all of which are essential for maintaining the normal integrity of the SCV compartment.

PLEKHM1 PH2 Domain Mutants Influence *Salmonella* Proliferation and Vacuole Morphology

Finally, we wanted to assess whether the PLEKHM1-PH2 domain mutations that influence the interaction with SifA are relevant for *Salmonella* proliferation and vacuole formation. We expressed shRNA-resistant PLEKHM1-WT, -ΔPH2, -E729A, -T730A, and -R769A in shRNA-depleted PLEKHM1 cells and performed gentamycin protection assays and confocal micrograph analysis of the SCV at 24 hr p.i. In PLEKHM1-WT-expressing cells, we observed PLEKHM1 colocalization with LAMP1 at distinct regions of the SCV (Figure 7A, closed arrowheads) and also to the remnants of Sifs (Figure 7A, open arrows). However, none of the PH2 domain mutants colocalized with LAMP1 at the SCV, and the characteristic "bag" of *Salmonella* was evident in all the mutants (Figures 7B–7D; quantified in Figure 7F; T730A data not shown). In the gentamycin protection assays, *Salmonella* proliferation in PLEKHM1-ΔPH2-reconstituted cells was approximately 50% reduced compared to PLEKHM1-WT, similar to the effect of PLEKHM1 depletion (Figure 7E). Thus, PLEKHM1 is a lysosomal adaptor protein that lies at a critical juncture between the host lysomembrane system and the *Salmonella* proliferative niche that when disrupted affects both proliferation and SCV morphology.

DISCUSSION

The *Salmonella* effector protein SifA is essential for the formation of Sifs (Stein et al., 1996) and the maintenance of *Salmonella* vacuoles (Beuzón et al., 2000). Accordingly, *Salmonella* lacking SifA are more frequently found in the host cytosol; although the underlying mechanism is not known, the bacteria are potentially released from the SCV due to membrane rupture. As SifA is critically involved in the formation of the membrane-consuming filamentous structures (Sifs), it is suggested that SifA somehow utilizes and redirects endogenous membrane sources for SCV biogenesis. One potential SifA target represents Rab7 as Sif formation depends on Rab7 function (Méresse et al., 1999). Yet, how SifA impinges on membrane trafficking events controlled by Rab7 remained enigmatic.

Herein, we characterized PLEKHM1, a multifunctional endocytic adaptor protein that can directly interact with the small GTPase Rab7, components of the HOPS complex, and *Salmonella* effector protein SifA. Formation of this complex would ensure a feedforward loop that would rapidly amplify GTP loading of Rab7 by HOPS complex at the membranes. PLEKHM1 was identified in complex with Rab7-GTP with known effectors like RUBICON, and loss of PLEKHM1 led to reduced Rab7-GTP in cells. Critically, all of these interactions intersect at the endolysosomal compartment, as loss of PLEKHM1 causes gross morphological changes in the SCV and limits the intracellular proliferation of *Salmonella*.

Cells harbor an intricate machinery for orchestrating the trafficking of cellular cargo to ensure that they end up in the right place at the right time—whether this is at the plasma membrane or degradation in the lysosomes. The large Rab family of small guanine nucleotide-binding proteins as well as the HOPS complex have a crucial role in regulating this process (McEwan et al., 2015). They can interact with effector proteins such as kinases, adaptors, tethering factors, and motor proteins, contributing to processes such as vesicle budding at the plasma membrane and transport, sorting of cargo, and fusion of vesicles such as endosome/lysosome or autophagosome/endosome/lysosome fusion (Balderhaar and Ungermann, 2013; Stenmark, 2009). Our study provides insights into how *Salmonella* (but potentially also other pathogens) hijacks the endogenous membrane trafficking machinery—represented by Rab7 and the HOPS complex—to establish a proliferative intracellular niche following cell invasion.

To date, the role of the HOPS complex in mammalian systems has been poorly addressed, while the majority of our

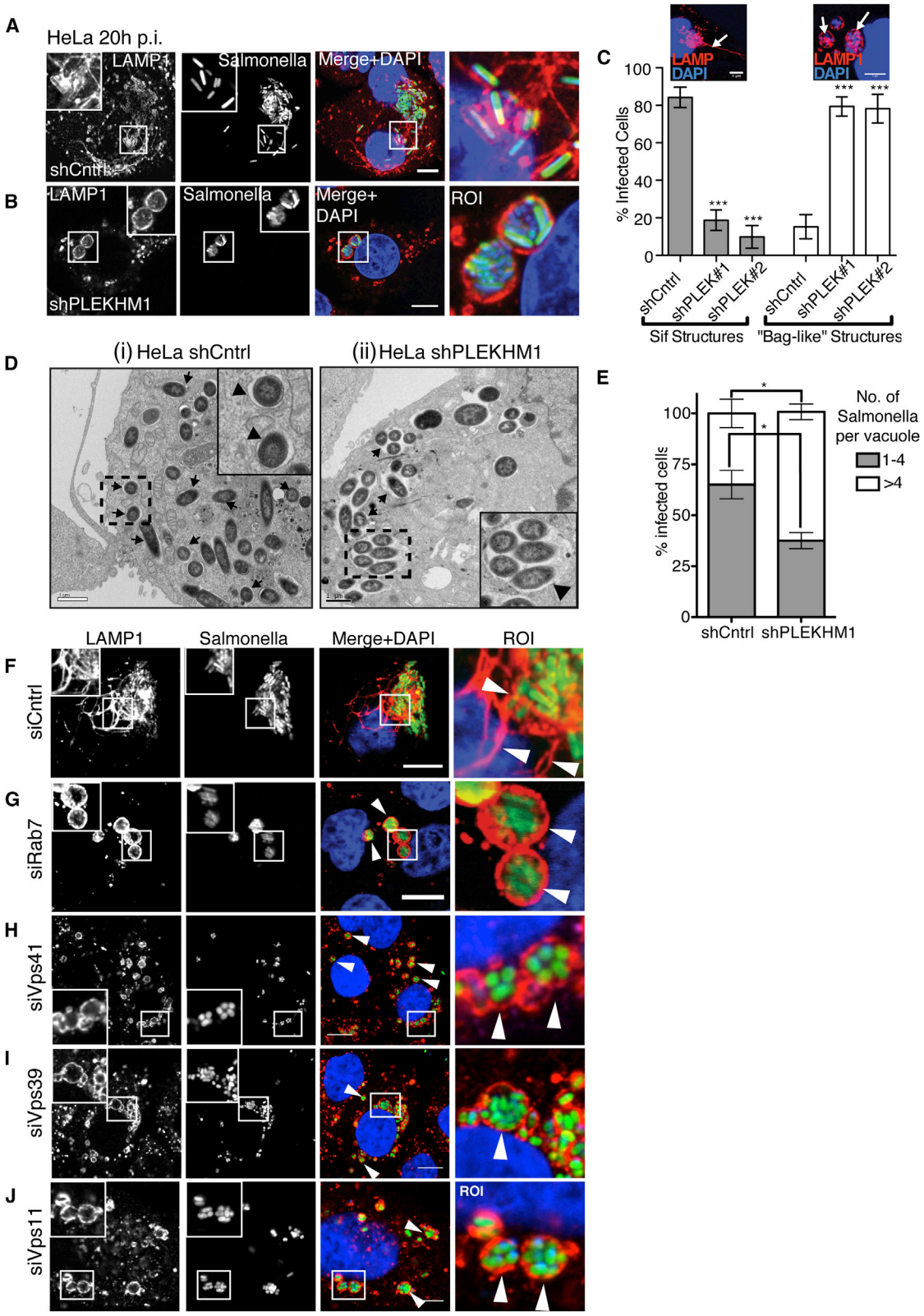

Figure 6. PLEKHM1 Depletion Causes Abnormal *Salmonella*-Containing Vacuoles

(A and B) (A) shRNA control or shPLEKHM1 (B) HeLa cells were infected with GFP-expressing WT *Salmonella* (SL1344-GFP; green) stained for endogenous LAMP1 (red) and DAPI (blue). Scale bar 10 μm.

(legend continued on next page)

knowledge stems from studies carried out in yeast. Although these studies led us to a vivid understanding of the molecular architecture of this complex and how it is organized in yeast (reviewed in Balderhaar and Ungermann, 2013), the complex composition in higher organisms is not yet fully elucidated. Specifically, despite clear evidence of Vps39 directly interacting with Rab7 (Ypt7) (Bröcker et al., 2012), there are conflicting reports of hVps39 interacting with Rab7 (Caplan et al., 2001; Rink et al., 2005) and RILP (Caplan et al., 2001; van der Kant et al., 2013). Conspicuously, yeast does not have any PLEKHM1 or RILP homologs, strongly suggesting that the mammalian system has potentially evolved so that HOPS can function in conjunction with Rab7-adaptor proteins in various endocytic pathways. Recently, there have been several functional studies addressing the role of mammalian HOPS complex and its adaptors. For example, a genetic screen identified 67 different mutations within all six HOPS complex genes that conferred a resistance to infection by the hemorrhagic-fever-causing Ebola virus, notably characterized by an arrest of viral membrane fusion and inhibition of escape from the lysosomal compartment (Carette et al., 2011). In addition, RILP has also been shown to interact with HOPS complex, and overexpression of HOPS-deficient binding mutants reduced Ebola virus infectivity by half (van der Kant et al., 2013). Currently, little is known of any involvement of HOPS complex during the *Salmonella* infection cycle. We provide evidence for a functional synergism between PLEKHM1, HOPS, and Rab7 in regulating the SCV. The absence of any of these components causes substantial deformation of the SCV and limited proliferation of multiple *Salmonella* within a single, enlarged vacuole. Interestingly, the lack of Sifs does not appear to completely inhibit the growth of *Salmonella* in a vacuole and may represent a functional redundancy for this structure with regards to overall survival in the cell.

The unique ability of PLEKHM1 is to act as a protein interaction platform coupling different pathways to the Rab7/HOPS complex. The *Salmonella* effector protein SifA apparently hijacks this hub by direct binding to PLEKHM1. SifA is a critical virulence factor that promotes continuous membrane exchange with the late endosomal/lysosomal compartment (Beuzón et al., 2000; Dumont et al., 2010; Méresse et al., 1999). SifA loss results in SCV membrane rupture and consequent exposure to the host cytosol due to the uncoordinated recruitment of effector proteins by SopD2 and SseJ (Ruiz-Albert et al., 2002; Schroeder et al., 2010), triggering the ubiquitin-dependent recruitment of the autophagic machinery to cytosolic *Salmonella* (Cemma et al., 2011; Rogov et al., 2013; Thurston et al., 2009; Wild et al., 2011; Zheng et al., 2009). Previously, it was unclear how SifA and other effectors coordinate membrane delivery and fusion with the SCV. For example, SifA is responsible for Rab7 recruitment but does not bind to it directly (Harrison et al., 2004), and RILP is absent from Sifs (Harrison et al., 2004); neither does it interact with SifA (Jackson et al., 2008). SKIP does bind to SifA, is essential for *Salmonella* pathogenesis, and, interestingly, interacts with Rab9 but not Rab7 (Boucrot et al., 2005; Diacovich et al., 2009; Dumont et al., 2010; Jackson et al., 2008; Ohlson et al., 2008). As such, SifA utilizes SKIP to subvert the Rab9-dependent retrograde trafficking of mannose-6-phosphate receptors and detoxifies lysosomes (McGourty et al., 2012). Recently, the HOPS subunit Vps41 together with LAMP1/2 and VAMP7 have been shown to act as a transport system for lysosome-associated membrane proteins (Pols et al., 2013). Importantly, these LAMP1 carriers act independently and in parallel to mannose-6-phosphate receptor transport (Pols et al., 2013). Indeed, Rab7 localized to these carriers, but it is unclear if Rab7 effector proteins are also present (Pols et al., 2013). However, these carriers would provide a clear source of membrane, devoid of M6PR, for the expanding SCV. The PLEKHM1/Rab7/HOPS complex is thus clearly essential for dynamic SCV compartment morphology, perhaps through the recruitment of membranes for SCV growth.

The formation of Sifs requires multiple *Salmonella* effector proteins, including SifA, SseF, SseJ, SopD2, SseG, and PipB2 (Brumell et al., 2002a; Kuhle et al., 2004), and the network can be distinguished by several different types of tubular networks—including *Salmonella*-induced SCAMP3 tubules (Mota et al., 2009) and LAMP1-negative tubules (Schroeder et al., 2010). Interestingly, a recent report showed high-resolution EM images of the SCV and the emanating Sif structures (Krieger et al., 2014), which revealed two distinct types of Sif; a double membrane and a single membrane (Type 2 and Type 1, respectively). PLEKHM1 could directly impinge on the formation of both types, as we do not see any Sifs in PLEKHM1-depleted cells. Alternatively, the absence of PLEKHM1/Rab7/HOPS may inhibit the partitioning of the SCV during bacterial replication. Therefore, the identified role of PLEKHM1 opens up a paradigm on how *Salmonella* manipulate the endolysosomal compartment: on the one hand detoxifying lysosomes through SifA/SKIP/Rab9 and on the other via the recruitment of the lysosomal membrane machinery by SifA/PLEKHM1/Rab7/HOPS, providing a stable intracellular proliferative niche.

In conclusion, this study provides a link between the important *Salmonella* effector protein SifA and Rab7-dependent biogenesis of Sifs and membrane dynamics. These observations

(C) Representative of images of Sif (left) and bag (right) structures and quantification of structures after 24 hr p.i. in shPlek and shCntrl HeLa cells. LAMP1 (red) and DAPI (blue) staining is shown. Arrows indicate relevant structures. Infected cells were scored to have either Sif or "bag" structures and were expressed as percentage of total infected cells. Error bars indicate mean ± SEM; n = 3 independent experiments. ***$p < 0.001$; unpaired t test compared to shCntrl.

(D) Representative EM images from shCntrl (left) or shPLEKHM1 (shPLEK#2) HeLa cells imaged at 20 hr p.i. Boxed area shown as enhancement. Arrows indicate vacuoles of interest. Scale bar 1 μm.

(E) Quantification of (D) 200 cell profiles per random section. Each infected cell observed was assigned to one of the following categories: vacuoles containing one to four bacteria or vacuoles containing greater than four bacteria. Error bars indicate mean ± SEM; n = 3 random sections from independent blocks. *$p < 0.03$ compared to shCntrl.

(F–J) (F) Representative confocal micrographs of siCntrl, (G) siRab7-, (H) siVps41-, (I) siVps39-, and (J) siVps11-depleted HeLa cells 20 hr p.i. with SL1344-GFP (green), stained with anti-LAMP1 (red) and DAPI (blue). Images are representative of n = 3 independent experiments. Boxed regions are enhanced in the panels labeled ROI. Arrows indicate structures of interest. Scale bars 10 μm.

See also Figure S7.

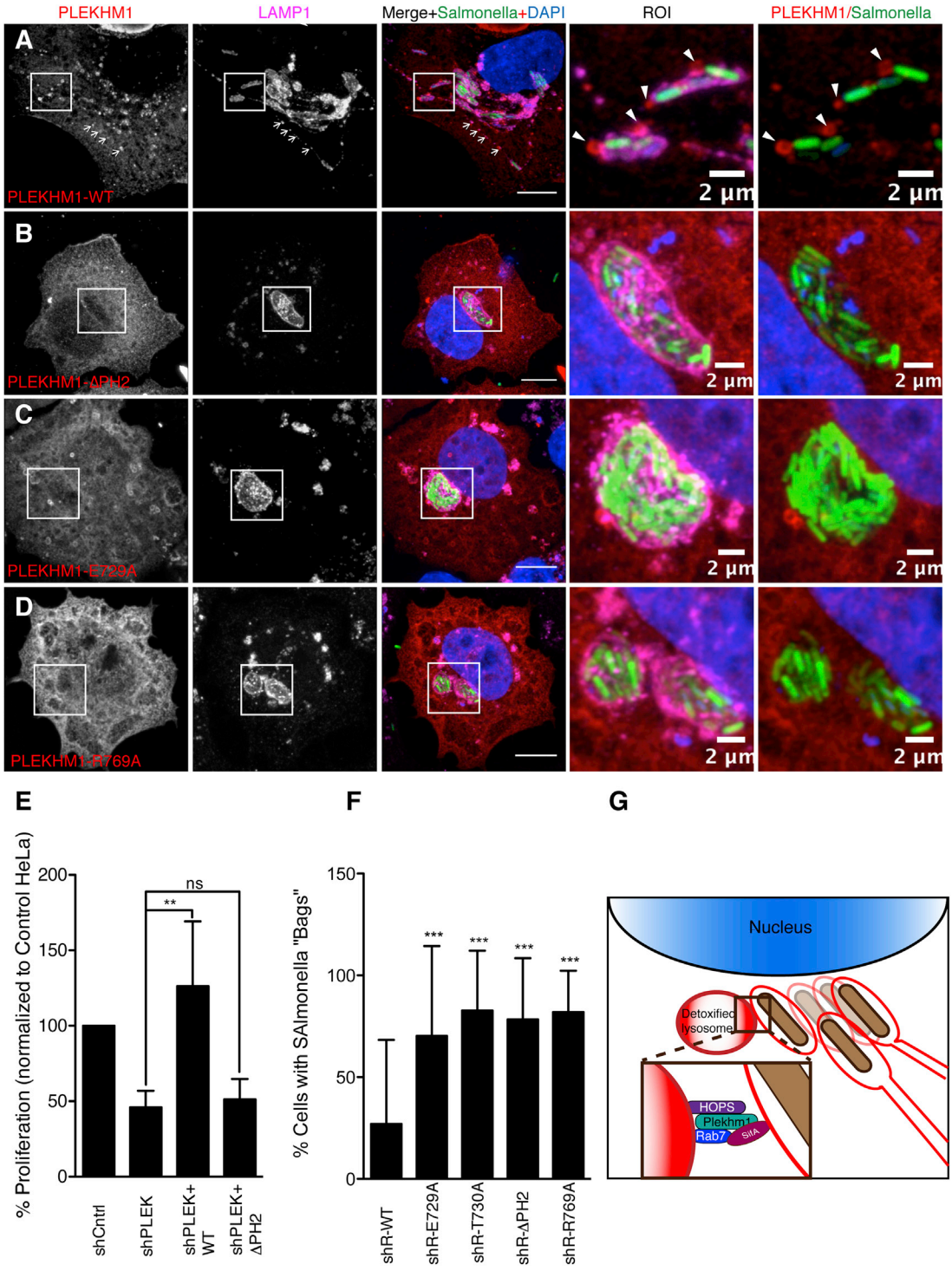

Figure 7. PLEKHM1 PH2 Domain Mutants Affect Salmonella Proliferation and Vacuole Morphology

(A–D) HeLa cells depleted of PLEKHM1 (shPLEK#1) were transiently reconstituted with shRNA-resistant PLEKHM1-WT (A), -ΔPH2 (B), E729A (C), and R769A (D); infected with SL1344-GFP WT Salmonella; and the SCVs were analyzed by confocal microscopy. Images shown are representative z stack reconstructions of infected cells. Scale bar 10 μm unless otherwise stated.

(E) Proliferation of Salmonella in shPLEKHM1 cells transiently overexpressing PLEKHM1 WT and PH2 domain mutant. Cfu counts calculated as fold 2 hr p.i. and expressed as a percentage of shCntrl HeLa cells. n = 4 mean ± SD.

(F) Quantification of percentage cells with Salmonella "bag" structure of (A)–(D). n = 60 cells per condition. Mean ± SD. ***$p < 0.002$, Student's t test compared to PLEKHM1-WT-expressing cells.

(G) Proposed model of how *Salmonella* recruit PLEKHM1/Rab7/HOPS by SifA to the SCV.

might also be relevant to the pathogenesis of other intracellular bacteria that reside in the pathogen-inhabited compartments like *Legionella spp.*, *Chlamydia* spp., *Coxiella* spp., *Bartonella* spp., *Francisella* spp., and many others. Thus, targeting of PLEKHM1 might be a potential strategy to interfere with the intracellular growth of pathogenic bacteria in the host cells.

EXPERIMENTAL PROCEDURES

Salmonella Infections

HeLa cells were plated at 3 × 10^5 cells in 6-well plates in Dulbecco's modified Eagle's medium (DMEM) with 10% FCS and antibiotics (penicillin and streptomycin). After 18 hr, media were changed to antibiotic-free medium, and cells were transfected with the indicated plasmids using Genejuice (Novagen). Infections with *Salmonella* were performed 24 hr after transfection. An overnight (stationary) culture of *Salmonella* was diluted 1:33 and bacteria were grown at 37°C for 3 hr until the OD600 was typically 1.5–2.0. *Salmonella (SL1344 and S12023)* infection was performed at a multiplicity of infection of 100. *Salmonella* were allowed to invade cells for 20 min. Afterward, media were replaced by DMEM containing 100 μg/ml gentamycin for 1 hr and replaced with DMEM containing 10% FBS and 20 μg/ml gentamycin. For cfu counts, cells were lysed in buffer (PBS with 0.1% Triton X-100) and plated on agar plates. For microscopy studies, cells were fixed in 4% paraformaldehyde for 20 min at room temperature, followed by washing with PBS containing 20 mM glycine, and processed for immunofluorescence. For siRNA experiments, HeLa cells (2.5 × 10^5) were transfected with siRNA using Lipofectamine RNAi Max (Thermo), and infection was performed 48–72 hr after knockdown. Macrophages were infected with an overnight (stationary) culture of SL1344 for 40 min. Mice were infected with some 500 cfu SL1344 in 100 μl PBS by tail-vein injection and sacrificed 6 days p.i. For reconstitution experiments, shRNA PLEKHM1-depleted HeLa cells were transfected with shRNA-resistant PLEKHM1-WT and PH2 domain mutants as indicated, 24 hr prior to infection. Cells were infected as above and either fixed for immunofluorescence analysis or lysed for cfu counts.

Mouse Strain and In Vivo Infections

Plekhm1 gene trap mice (B6;129S5-Plekhm1$^{Gt(OST201689)Lex}$/Orl; LEXKO-0354) were acquired from Lexicon Pharmaceuticals through the Wellcome Trust Access to Mutant Mouse Resources (UK). These mice had been generated by retrovirally transducing 129SV embryonic stem cells with a neomycin cassette targeted between exons 1 and 2 of *Plekhm1* gene. The mice were subsequently backcrossed ten generations into C57BL/6. Heterozygous mice (*Plekhm1*$^{+/-}$) were mated and embryos isolated at embryonic day 13.5 (E13.5). Isolated MEFs were then infected at typically low passages (P3–P5) cells. Genotypes were confirmed both by genotyping, using primers designed specifically overlapping genetrap insertion (KO), and by western blot. Infection of mice was carried out by intravenous injection of 1,300 cfu *Salmonella* (strain SL1344), mice were sacrificed 5 days p.i., their spleens and livers harvested, cfu counts analyzed. All animal experiments were approved (license 2239, Kantonales Veterinäramt Basel-Stadt) and performed according to local guidelines (Tierschutz-Verordnung, Basel-Stadt) and the Swiss animal protection law (Tierschutz-Gesetz).

Transmission Electron Microscopy

(1) Preparation of Cells

Cell culture media was removed and cell fixed in 4% paraformaldehyde and 0.1% glutaraldehyde in 0.1 M PHEM buffer for 3 hr at room temperature. Cells were washed and incubated with 50 mM glycine/100 mM PHEM for 10 min, washed in 1% BSA in 100 mM cacodylate buffer, and pelleted. PFA was removed with 100 mM cacodylate buffer and cells subsequently fixed in 2.5% glutaraldehyde for 1 hr at room temperature. The resulting pellet was divided and incubated 1 hr at room temperature with 1% osmium in 100 mM cacodylate buffer. Samples were washed with deionized water and en bloc stained with 1% uranylacetate for 1 hr at room temperature in the dark. Graded dehydration in ethanol was followed by embedding in Epon resin and ultrathin sections of ca. One hundred nanometer thicknesses were cut using an EM UC7 ultramicrotome (Leica AG, Wetzlar, Germany) and poststained using 2% uranylacetate and Reynolds lead citrate.

(2) Transmission Electron Microscopy

Three individual blocks of both shControl and shPLEKHM1 cells were sectioned and evaluated by TEM. From each block, one random 100 nm was analyzed using a Zeiss TEM operated at 80 kV. The random sections were screened in a systematic boustrophedonical way using a magnification of 1,000×. A total of 200 cell profiles were analyzed per random section. Each cell observed was assigned to one of the following categories: no *Salmonella*-containing vacuoles, vacuoles containing one to four bacteria, vacuoles containing five to ten bacteria, and vacuoles containing >10 bacteria.

MEF Generation

Plekhm1 knockout mice were generated by Lexicon genetics using retroviral insertion of a genetrap between exons 1 and 2 of mouse Plekhm1 gene. Embryos were isolated from a Plekhm1 heterozygous breeding at day E13.5. Embryos were dissected, trypsinized, and grown to confluence. Genotypes were confirmed both by genotyping using primers designed specifically overlapping genetrap insertion (KO) and by western blot. Infections were carried out at typically low passages (P3–P5) cells.

Statistical Analysis

Results were analyzed using unpaired Student's t test using Graphpad (Prism) software.

Detailed experimental procedures can be found in the Supplemental Information.

SUPPLEMENTAL INFORMATION

Supplemental Information includes seven figures, three tables, four movies, and Supplemental Experimental Procedures and can be found with this article online at http://dx.doi.org/10.1016/j.chom.2014.11.011.

ACKNOWLEDGMENTS

We would like to acknowledge Anja Bremm and Margaret Frame for critical reading of the manuscript and valuable insights. We would like to thank S. Wahl and J. Madlung for sample preparation and MS measurement. The mCherry-LAMP1 was a kind gift from J. Lippincott-Schwartz, and the SifA and SKIP construct was a generous gift from S. Meresse. The anti-LAMP1 and LAMP2 antibody developed by J.T. August was obtained from the Developmental Studies Hybridoma Bank developed under the auspices of the NICHD and maintained by The University of Iowa, Department of Biology. K.R. is a Heisenberg professor of the DFG (RA1739/4-1), a BIS-PLUS3 fellow, and a GRC fellow. This work was supported by grants from the Flemish FWO G.0065.10N to W.V.H., Arthritis Research UK (grant number 19379) to F.P.C. and M.H.H., Deutsche Forschungsgemeinschaft (DI 931/3-1; DI 931/11-1), the Cluster of Excellence "Macromolecular Complexes" of the Goethe University Frankfurt (EXC115), LOEWE grant Ub-Net and LOEWE Centrum for Gene and Cell therapy Frankfurt, and the European Research Council/ERC grant agreement n° 250241-LineUb to I.D.; Landesstiftung Baden-Württemberg Stiftung and PRIME-XS to B.M. and Swiss National Foundation (31003A-121834), SystemsX.ch (RTD project "BattleX") to D.B.

Received: May 5, 2014
Revised: October 21, 2014
Accepted: November 14, 2014
Published: December 11, 2014

REFERENCES

Balderhaar, H.J., and Ungermann, C. (2013). CORVET and HOPS tethering complexes - coordinators of endosome and lysosome fusion. J. Cell Sci. *126*, 1307–1316.

Berón, W., Gutierrez, M.G., Rabinovitch, M., and Colombo, M.I. (2002). Coxiella burnetii localizes in a Rab7-labeled compartment with autophagic characteristics. Infect. Immun. *70*, 5816–5821.

Beuzón, C.R., Méresse, S., Unsworth, K.E., Ruíz-Albert, J., Garvis, S., Waterman, S.R., Ryder, T.A., Boucrot, E., and Holden, D.W. (2000). Salmonella maintains the integrity of its intracellular vacuole through the action of SifA. EMBO J. *19*, 3235–3249.

Birmingham, C.L., Smith, A.C., Bakowski, M.A., Yoshimori, T., and Brumell, J.H. (2006). Autophagy controls Salmonella infection in response to damage to the Salmonella-containing vacuole. J. Biol. Chem. *281*, 11374–11383.

Boucrot, E., Henry, T., Borg, J.P., Gorvel, J.P., and Méresse, S. (2005). The intracellular fate of Salmonella depends on the recruitment of kinesin. Science *308*, 1174–1178.

Bröcker, C., Kuhlee, A., Gatsogiannis, C., Balderhaar, H.J., Hönscher, C., Engelbrecht-Vandré, S., Ungermann, C., and Raunser, S. (2012). Molecular architecture of the multisubunit homotypic fusion and vacuole protein sorting (HOPS) tethering complex. Proc. Natl. Acad. Sci. USA *109*, 1991–1996.

Brumell, J.H., Goosney, D.L., and Finlay, B.B. (2002a). SifA, a type III secreted effector of Salmonella typhimurium, directs Salmonella-induced filament (Sif) formation along microtubules. Traffic *3*, 407–415.

Caplan, S., Hartnell, L.M., Aguilar, R.C., Naslavsky, N., and Bonifacino, J.S. (2001). Human Vam6p promotes lysosome clustering and fusion in vivo. J. Cell Biol. *154*, 109–122.

Carette, J.E., Raaben, M., Wong, A.C., Herbert, A.S., Obernosterer, G., Mulherkar, N., Kuehne, A.I., Kranzusch, P.J., Griffin, A.M., Ruthel, G., et al. (2011). Ebola virus entry requires the cholesterol transporter Niemann-Pick C1. Nature *477*, 340–343.

Cemma, M., Kim, P.K., and Brumell, J.H. (2011). The ubiquitin-binding adaptor proteins p62/SQSTM1 and NDP52 are recruited independently to bacteria-associated microdomains to target Salmonella to the autophagy pathway. Autophagy *7*, 341–345.

Diacovich, L., Dumont, A., Lafitte, D., Soprano, E., Guilhon, A.A., Bignon, C., Gorvel, J.P., Bourne, Y., and Méresse, S. (2009). Interaction between the SifA virulence factor and its host target SKIP is essential for Salmonella pathogenesis. J. Biol. Chem. *284*, 33151–33160.

Dumont, A., Boucrot, E., Drevensek, S., Daire, V., Gorvel, J.P., Poüs, C., Holden, D.W., and Méresse, S. (2010). SKIP, the host target of the Salmonella virulence factor SifA, promotes kinesin-1-dependent vacuolar membrane exchanges. Traffic *11*, 899–911.

Gomes, L.C., and Dikic, I. (2014). Autophagy in antimicrobial immunity. Mol. Cell *54*, 224–233.

Gorvel, J.P., and Meresse, S. (2001). Maturation steps of the *Salmonella*-containing vacuole. Microbes Infect. *3*, 1299–1303.

Guignot, J., Caron, E., Beuzón, C., Bucci, C., Kagan, J., Roy, C., and Holden, D.W. (2004). Microtubule motors control membrane dynamics of Salmonella-containing vacuoles. J. Cell Sci. *117*, 1033–1045.

Harrison, R.E., Brumell, J.H., Khandani, A., Bucci, C., Scott, C.C., Jiang, X., Finlay, B.B., and Grinstein, S. (2004). Salmonella impairs RILP recruitment to Rab7 during maturation of invasion vacuoles. Mol. Biol. Cell *15*, 3146–3154.

Jackson, L.K., Nawabi, P., Hentea, C., Roark, E.A., and Haldar, K. (2008). The Salmonella virulence protein SifA is a G protein antagonist. Proc. Natl. Acad. Sci. USA *105*, 14141–14146.

Korolchuk, V.I., Saiki, S., Lichtenberg, M., Siddiqi, F.H., Roberts, E.A., Imarisio, S., Jahreiss, L., Sarkar, S., Futter, M., Menzies, F.M., et al. (2011). Lysosomal positioning coordinates cellular nutrient responses. Nat. Cell Biol. *13*, 453–460.

Krieger, V., Liebl, D., Zhang, Y., Rajashekar, R., Chlanda, P., Giesker, K., Chikkaballi, D., and Hensel, M. (2014). Reorganization of the endosomal system in Salmonella-infected cells: the ultrastructure of Salmonella-induced tubular compartments. PLoS Pathog. *10*, e1004374.

Kuhle, V., Jäckel, D., and Hensel, M. (2004). Effector proteins encoded by Salmonella pathogenicity island 2 interfere with the microtubule cytoskeleton after translocation into host cells. Traffic *5*, 356–370.

McEwan, D.G., Popovic, D., Gubas, A., Terawaki, S., Suzuki, H., et al. (2015). PLEKHM1 regulates autophagosome-lysosome fusion through HOPS complex and LC3/GABARAP proteins. Mol. Cell *57*, this issue, 39–54.

McGourty, K., Thurston, T.L., Matthews, S.A., Pinaud, L., Mota, L.J., and Holden, D.W. (2012). Salmonella inhibits retrograde trafficking of mannose-6-phosphate receptors and lysosome function. Science *338*, 963–967.

Méresse, S., Steele-Mortimer, O., Finlay, B.B., and Gorvel, J.P. (1999). The rab7 GTPase controls the maturation of Salmonella typhimurium-containing vacuoles in HeLa cells. EMBO J. *18*, 4394–4403.

Mota, L.J., Ramsden, A.E., Liu, M., Castle, J.D., and Holden, D.W. (2009). SCAMP3 is a component of the Salmonella-induced tubular network and reveals an interaction between bacterial effectors and post-Golgi trafficking. Cell. Microbiol. *11*, 1236–1253.

Nordmann, M., Cabrera, M., Perz, A., Bröcker, C., Ostrowicz, C., Engelbrecht-Vandré, S., and Ungermann, C. (2010). The Mon1-Ccz1 complex is the GEF of the late endosomal Rab7 homolog Ypt7. Curr. Biol. *20*, 1654–1659.

Ohlson, M.B., Huang, Z., Alto, N.M., Blanc, M.P., Dixon, J.E., Chai, J., and Miller, S.I. (2008). Structure and function of Salmonella SifA indicate that its interactions with SKIP, SseJ, and RhoA family GTPases induce endosomal tubulation. Cell Host Microbe *4*, 434–446.

Pankiv, S., Alemu, E.A., Brech, A., Bruun, J.A., Lamark, T., Overvatn, A., Bjørkøy, G., and Johansen, T. (2010). FYCO1 is a Rab7 effector that binds to LC3 and PI3P to mediate microtubule plus end-directed vesicle transport. J. Cell Biol. *188*, 253–269.

Papini, E., de Bernard, M., Milia, E., Bugnoli, M., Zerial, M., Rappuoli, R., and Montecucco, C. (1994). Cellular vacuoles induced by Helicobacter pylori originate from late endosomal compartments. Proc. Natl. Acad. Sci. USA *91*, 9720–9724.

Patel, J.C., and Galán, J.E. (2005). Manipulation of the host actin cytoskeleton by Salmonella—all in the name of entry. Curr. Opin. Microbiol. *8*, 10–15.

Peralta, E.R., Martin, B.C., and Edinger, A.L. (2010). Differential effects of TBC1D15 and mammalian Vps39 on Rab7 activation state, lysosomal morphology, and growth factor dependence. J. Biol. Chem. *285*, 16814–16821.

Pols, M.S., van Meel, E., Oorschot, V., ten Brink, C., Fukuda, M., Swetha, M.G., Mayor, S., and Klumperman, J. (2013). hVps41 and VAMP7 function in direct TGN to late endosome transport of lysosomal membrane proteins. Nat. Commun. *4*, http://dx.doi.org/10.1038/ncomms2360.

Ramsden, A.E., Holden, D.W., and Mota, L.J. (2007). Membrane dynamics and spatial distribution of Salmonella-containing vacuoles. Trends Microbiol. *15*, 516–524.

Rink, J., Ghigo, E., Kalaidzidis, Y., and Zerial, M. (2005). Rab conversion as a mechanism of progression from early to late endosomes. Cell *122*, 735–749.

Rogov, V.V., Suzuki, H., Fiskin, E., Wild, P., Kniss, A., Rozenknop, A., Kato, R., Kawasaki, M., McEwan, D.G., Löhr, F., et al. (2013). Structural basis for phosphorylation-triggered autophagic clearance of Salmonella. Biochem. J. *454*, 459–466.

Ruiz-Albert, J., Yu, X.J., Beuzón, C.R., Blakey, A.N., Galyov, E.E., and Holden, D.W. (2002). Complementary activities of SseJ and SifA regulate dynamics of the Salmonella typhimurium vacuolar membrane. Mol. Microbiol. *44*, 645–661.

Schroeder, N., Henry, T., de Chastellier, C., Zhao, W., Guilhon, A.A., Gorvel, J.P., and Méresse, S. (2010). The virulence protein SopD2 regulates membrane dynamics of Salmonella-containing vacuoles. PLoS Pathog. *6*, e1001002.

Seaman, M.N., Harbour, M.E., Tattersall, D., Read, E., and Bright, N. (2009). Membrane recruitment of the cargo-selective retromer subcomplex is catalysed by the small GTPase Rab7 and inhibited by the Rab-GAP TBC1D5. J. Cell Sci. *122*, 2371–2382.

Shahnazari, S., Yen, W.L., Birmingham, C.L., Shiu, J., Namolovan, A., Zheng, Y.T., Nakayama, K., Klionsky, D.J., and Brumell, J.H. (2010). A diacylglycerol-dependent signaling pathway contributes to regulation of antibacterial autophagy. Cell Host Microbe *8*, 137–146.

Steele-Mortimer, O., Méresse, S., Gorvel, J.P., Toh, B.H., and Finlay, B.B. (1999). Biogenesis of Salmonella typhimurium-containing vacuoles in epithelial

cells involves interactions with the early endocytic pathway. Cell. Microbiol. *1*, 33–49.

Stein, M.A., Leung, K.Y., Zwick, M., Garcia-del Portillo, F., and Finlay, B.B. (1996). Identification of a Salmonella virulence gene required for formation of filamentous structures containing lysosomal membrane glycoproteins within epithelial cells. Mol. Microbiol. *20*, 151–164.

Stenmark, H. (2009). Rab GTPases as coordinators of vesicle traffic. Nat. Rev. Mol. Cell Biol. *10*, 513–525.

Sun, J., Deghmane, A.E., Bucci, C., and Hmama, Z. (2009). Detection of activated Rab7 GTPase with an immobilized RILP probe. Methods Mol. Biol. *531*, 57–69.

Sun, Q., Westphal, W., Wong, K.N., Tan, I., and Zhong, Q. (2010). Rubicon controls endosome maturation as a Rab7 effector. Proc. Natl. Acad. Sci. USA *107*, 19338–19343.

Tabata, K., Matsunaga, K., Sakane, A., Sasaki, T., Noda, T., and Yoshimori, T. (2010). Rubicon and PLEKHM1 negatively regulate the endocytic/autophagic pathway via a novel Rab7-binding domain. Mol. Biol. Cell *21*, 4162–4172.

Thurston, T.L., Ryzhakov, G., Bloor, S., von Muhlinen, N., and Randow, F. (2009). The TBK1 adaptor and autophagy receptor NDP52 restricts the proliferation of ubiquitin-coated bacteria. Nat. Immunol. *10*, 1215–1221.

van der Kant, R., Fish, A., Janssen, L., Janssen, H., Krom, S., Ho, N., Brummelkamp, T., Carette, J., Rocha, N., and Neefjes, J. (2013). Late endosomal transport and tethering are coupled processes controlled by RILP and the cholesterol sensor ORP1L. J. Cell Sci. *126*, 3462–3474.

Via, L.E., Deretic, D., Ulmer, R.J., Hibler, N.S., Huber, L.A., and Deretic, V. (1997). Arrest of mycobacterial phagosome maturation is caused by a block in vesicle fusion between stages controlled by rab5 and rab7. J. Biol. Chem. *272*, 13326–13331.

Wild, P., Farhan, H., McEwan, D.G., Wagner, S., Rogov, V.V., Brady, N.R., Richter, B., Korac, J., Waidmann, O., Choudhary, C., et al. (2011). Phosphorylation of the autophagy receptor optineurin restricts Salmonella growth. Science *333*, 228–233.

Zheng, Y.T., Shahnazari, S., Brech, A., Lamark, T., Johansen, T., and Brumell, J.H. (2009). The adaptor protein p62/SQSTM1 targets invading bacteria to the autophagy pathway. J. Immunol. *183*, 5909–5916.